Journal for Geometry and Graphics
Volume 3 (1999), No. 2, 121–139

Reflections on Spheres and Cylinders of Revolution

Georg Glaeser

Institute for Architecture, University of Applied Arts Vienna
Oskar Kokoschka-Platz 2, A-1010 Wien, Austria
email: georg.glaeser@uni-ak.ac.at

Abstract. In computer graphics, it is often an advantage to calculate reflections directly, especially when the application is time-critical or when line graphics have to be displayed. We specify formulas and parametric equations for the reflection on spheres and cylinders of revolution. The manifold of all reflected rays is the normal congruence of an algebraic surface of order four. Their catacaustic surfaces are given explicitly. The calculation of the reflex of a space point leads to an algebraic equation of order four. The up to four practical solutions are calculated exactly and efficiently. The generation of reflexes of straight lines is optimized. Finally, reflexes of polygons are investigated, especially their possible overlappings. Such reflexes are the key for the reflection of polyhedra and curved surfaces. We describe in detail how to display their contours.

Key Words: Reflection, curved perspectives, caustic, normal congruence, specular points, real-time rendering.

MSC 1994: 51N05, 53A04, 68U05, 65Y25.

1. Introduction

Reflections play a central role in many applications of architecture, fine arts, photography, and of course in computer graphics itself. Especially the reflection on curved surfaces is a challenge. To give an example in architecture, we use the so-called “Haas-Haus” in Vienna ([12]). Its surface reflects St. Stephen’s cathedral and other historical buildings (Fig. 1). In contrast to reflections on planar surfaces, one can change the viewing position (walk around the building) and will always see the image (reflex) of the cathedral. The architect put an emphasis on the exact — and therefore much more expensive — production of the reflecting cylinder of revolution.

In computer graphics reflections are commonly rendered by ray tracing ([7]). The image is built up pixel by pixel in calcutation steps that are independent from each other. For each pixel, the following algorithm has to be applied:

ISSN 1433-8157/\$ 2.50

Through the center of each pixel, we shoot a projection ray ("forward ray tracing"). It may hit the scene in a frontmost point R. If the hit surface Φ is a reflecting surface, the projection ray is reflected according to the laws of optics and is followed recursively: When it hits the objects of the scene in a frontmost point S, the color of this object influences the color of the corresponding pixel, etc.

In this paper we proceed the other way round ("backward ray tracing", [1], [22]): Given a surface Φ, the eye point E and an arbitrary space point S, we are looking for a light ray $s \ni S$ that runs through E after being reflected on Φ in a "reflex" $R \in \Phi$. (Especially when S is a point light source, R is a specular point on Φ.) The point R is of course harder to find. Even in the simplest special cases we have to solve an algebraic equation of a higher degree.

Figure 1: "Haas-Haus"

The general geometric theory of reflections — especially its algebraic characterizations — were investigated decades ago (e.g., in [14]). It has not been applied much in computer graphics, though, because ray tracing and the radiosity method ([4]) could solve the problem in general. In this paper we will deduce very time-saving solutions for certain special cases. E.g., we specify formulas for the calculation of reflexes of points and straight lines. They are the key for displaying reflexes of polygons and curved (triangulated) surfaces.

The direct computation of reflexes is important (or even necessary)

- when we have to know the exact position of a reflex on a curved surface. The common methods will solve this problem only approximately and with great effort, since we have to render whole parts of the image.
- for the photo-realistic rendering of scenes with specular surfaces: The exact position of specular points (reflexes of point light sources) helps to speed up complex computations. Ordinary ray tracing, e.g., cannot take into account such complex lighting situations ([15]).
- for the real-time rendering of specular primitives like spheres and cylinders of revolution. When the exact position of the specular points are known, hardware supported GOURAUD-shading ([11]) can be applied efficiently (the corresponding polygonizations of such surfaces were adapted in the drawing routines of the latest version of the geometric programming package [9]).
- for the creation of line graphics including reflections (e.g., Fig. 3). In general, line graphics are not supported by the common rendering algorithms, and if they are, then only with "pixel accuracy". With the use of corresponding formulas, line graphics can be created very efficiently and independently of the screen resolution (including contours of curved sufaces).

We have to obey the following simple physical laws of reflection (Fig. 2):

1. The incoming light ray SR, the reflected light ray RE and the surface normal n in R are coplanar,
2. the incidence angles ζ_1 and ζ_2 of SR and RE are equal.

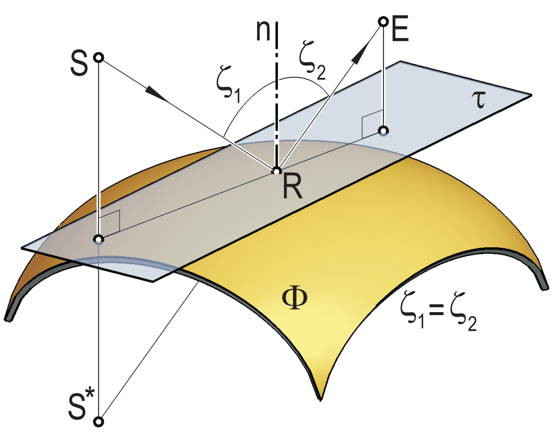

Figure 2: The laws of reflection

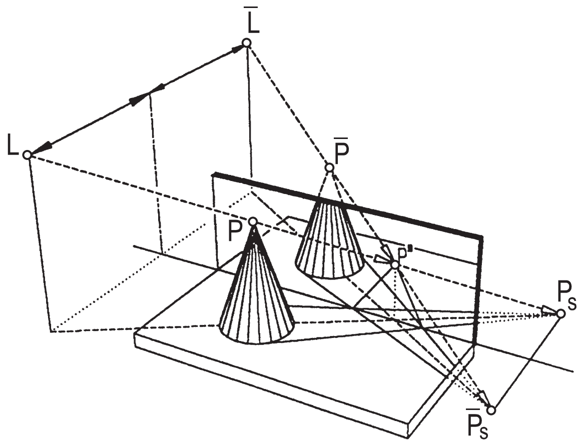

Figure 3: Reflection on a plane

The *reflection on a plane* can be easily calculated. We replace the surface Φ by its tangent plane $\tau \ni R$ (Fig. 2). When we reflect the point S on τ, we get a point S^*. The desired point R is then the intersection of ES^* and τ. Thus, the task is linear.

Scenes with reflections on planes can be displayed in real time without the use of ray tracing ([8]): Each reflecting plane induces a virtual reflected scene that can be seen through the "mirror window" (Fig. 3). It also induces, however, an additional light source that shines through the mirror window. Thus, the lightning situation complicates *exponentially* with the number of reflecting planes.

When Φ is curved, the solution of the problem soon becomes so complicated that human imagination hardly can judge whether a computer generated image is correct or not.

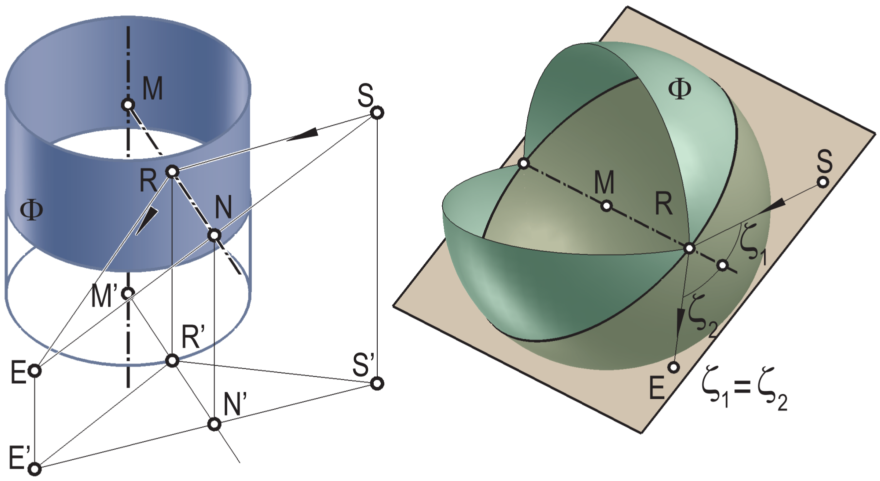

Figure 4: Special cases for Φ

In the following, we will only deal with the simplest two non-trivial cases, namely the reflection on a sphere $\Phi_\varkappa$ and a cylinder of revolution Φ_ζ. Fig. 4 shows that these two cases can be reduced to the two-dimensional case of the reflection on a circle: When Φ is a cylinder of revolution, we just have to look at its normal projection in the direction of the cylinder's axis, and when Φ is a sphere, we look at the situation in a plane through the sphere's center.

Reflections on circles have already very early been of interest. The problem was treated by Ptolemy (about AD 150), and it is known as "Alhazen's Problem" after the Arab scholar Ibn al-Haytham who wrote extensively about it almost exactly 1000 years ago ([17]). Due to its complexity, the problem could not be solved explicitly at that time. Caustics which result from multiple reflections on a circle have been investigated, e.g., by [13] and [21].

2. Reflection on a circle

In the following, let S, E, R and M denote points of two-space. Let the circle k (center M, radius $\mathbf{r}$) be the top view of a reflecting cylinder of revolution or the intersection circle of the reflecting sphere with the plane MES. M is chosen as the origin of a Cartesian coordinate system with E on the x-axis ($\overline{ME} = \mathbf{e}$). R and S may have the coordinates $R(r_x, r_y)$ (with $r_x^2 + r_y^2 = \mathbf{r}^2$) and $S(s_x, s_y)$.

The corresponding position vectors are $\vec{e} = \begin{pmatrix} \mathbf{e} \\ 0 \end{pmatrix}$, $\vec{r} = \begin{pmatrix} r_x \\ r_y \end{pmatrix}$ and $\vec{s} = \begin{pmatrix} s_x \\ s_y \end{pmatrix}$.

Definition: In the following we will use the abbreviation $\mathcal{R}[k; E]$ when we mean a reflection on a circle k with respect to the eye point E. The reflexes of a point S (a line c, etc.) will be denoted by $\mathcal{R}[k; E](S)$ ($\mathcal{R}[k; E](c)$, etc.). In the same way we will speak of $\mathcal{R}[\Phi_\varkappa; E]$ and $\mathcal{R}[\Phi_\zeta; E]$, when we mean the reflection on a sphere $\Phi_\varkappa$ and a cylinder Φ_ζ.

2.1. The calculation of the reflexes of a point

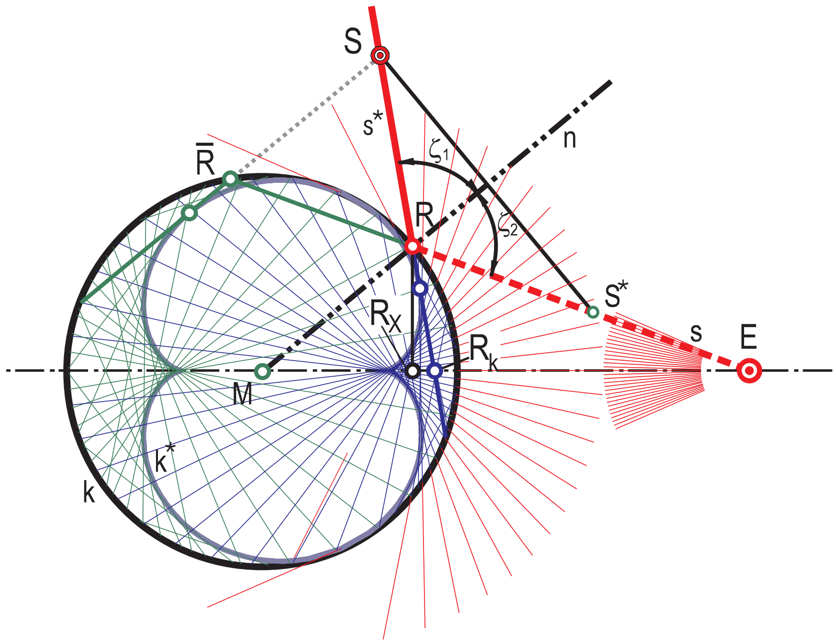

Figure 5: Catacaustic of the reflection congruence

Consider a ray $s \ni E$ that intersects k (Fig. 5). In the two intersection points R and $\overline{R}$ of k and s we theoretically have two reflected rays (reflection on the inside and on the outside).

The set of all reflected rays envelopes a curve k^*, the so-called *catacaustic*. Such curves were first studied by Huygens and Tschirnhausen around 1678.

We now filter those rays that — really or virtually — run through S. They are the tangents from S at k^* (see also Fig. 8).

The circle's normal n (the radial ray MR) is given by the vector equation

$$\vec{n}\vec{x} = 0 \text{ with } \vec{n} = \frac{1}{\mathbf{r}}\begin{pmatrix} r_y \\ -r_x \end{pmatrix} \text{ and } \vec{x} = \begin{pmatrix} x \\ y \end{pmatrix}$$

The distance of the point S from it is

$$d = \vec{n}\,\vec{s} = \frac{1}{\mathbf{r}}(r_y s_x - r_x s_y). \tag{1}$$

The point S^* symmetrical to S with respect to n is given through the vector equation

$$\overrightarrow{s^*} = \vec{s} - 2d\,\vec{n} = \begin{pmatrix} s_x - \frac{2d}{\mathbf{r}} r_y \\ s_y + \frac{2d}{\mathbf{r}} r_x \end{pmatrix}.$$

The reflected ray RS^* has thus the parametric equation

$$\vec{x} = \vec{r} + t(\overrightarrow{s^*} - \vec{r}) = \vec{r} + \lambda \begin{pmatrix} s_x - \frac{2d}{\mathbf{r}} r_y - r_x \\ s_y + \frac{2d}{\mathbf{r}} r_x - r_y \end{pmatrix}.$$

The corresponding parameter-free equation is

$$\begin{pmatrix} s_y + \frac{2d}{\mathbf{r}} r_x - r_y \\ -s_x + \frac{2d}{\mathbf{r}} r_y + r_x \end{pmatrix} \vec{x} = \begin{pmatrix} s_y + \frac{2d}{\mathbf{r}} r_x - r_y \\ -s_x + \frac{2d}{\mathbf{r}} r_y + r_x \end{pmatrix} \begin{pmatrix} r_x \\ r_y \end{pmatrix} = \underbrace{r_x s_y - r_y s_x}_{-\mathbf{r}d} + \underbrace{\frac{2d}{\mathbf{r}}(r_x^2 + r_y^2)}_{2\mathbf{r}d} = \mathbf{r}d.$$

Now E has to coincide with the reflected ray:

$$\begin{pmatrix} s_y + \frac{2d}{\mathbf{r}} r_x - r_y \\ -s_x + \frac{2d}{\mathbf{r}} r_y + r_x \end{pmatrix} \begin{pmatrix} \mathbf{e} \\ 0 \end{pmatrix} = \mathbf{r}d.$$

This leads to the condition

$$\mathbf{e}(s_y + \frac{2d}{\mathbf{r}} r_x - r_y) = \mathbf{r}d \quad \text{with} \quad \mathbf{r}d = r_y s_x - r_x s_y. \tag{2}$$

For better understanding, we substitute $x = r_x$ and $y = r_y$ $(x^2 + y^2 = \mathbf{r}^2)$. Then (2) shows as

$$\mathbf{e}[s_y + \frac{2}{\mathbf{r}^2}(s_x y - s_y x)x - y] = s_x y - s_y x,$$

which allows to explicitly calculate y:

$$y = s_y \frac{2\mathbf{e}x^2 - \mathbf{r}^2(x+\mathbf{e})}{2\mathbf{e}s_x x - \mathbf{r}^2(s_x+\mathbf{e})} \qquad (3)$$

(3) describes a hyperbola $h \ni S$ (Fig. 6). One asymptote is parallel to the y-axis, the other one is parallel to the radial ray through S. The intersection points D_1 and D_2 with the x-axis (the ray EM) are independent from S and have the x-values

$$x_{1,2} = \frac{\mathbf{r}}{4\mathbf{e}}(\mathbf{r} \pm \sqrt{\mathbf{r}^2 + 8\mathbf{e}^2}). \qquad (4)$$

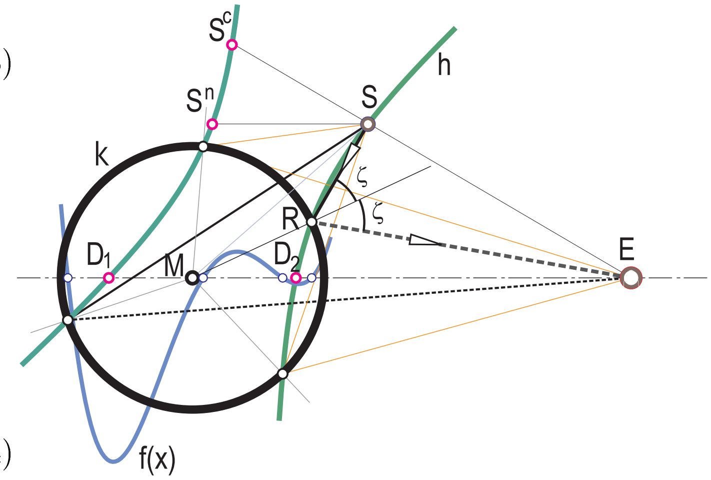

Figure 6: Geometric solution

The residual intersection points S^n and S^c with the x-parallels through S and the projection ray ES respectively have the x-values $\frac{\mathbf{r}^2}{2\mathbf{e}}$ or $\frac{\mathbf{r}^2}{\mathbf{e}}$ respectively.

The hyperbola intersects the circle k ($x^2 + y^2 = \mathbf{r}^2$) in four points that correspond to the four tangents at the catacaustic k^* through S (Fig. 8). Thus the problem cannot be solved by ruler and compass ([17]).

For all solutions $R = \mathcal{R}[k; E](S)$, we have

$$x^2 + y^2 - \mathbf{r}^2 = 0 \;\Rightarrow\; x^2 + [s_y \frac{2\mathbf{e}x^2 - \mathbf{r}^2(x+\mathbf{e})}{2\mathbf{e}s_x x - \mathbf{r}^2(s_x+\mathbf{e})}]^2 - \mathbf{r}^2 = 0$$

or

$$f(x) = (x^2 - \mathbf{r}^2)[2\mathbf{e}s_x x - \mathbf{r}^2(s_x+\mathbf{e})]^2 + s_y^2[2\mathbf{e}x^2 - \mathbf{r}^2(x+\mathbf{e})]^2 = 0$$

This leads to the following

Theorem 1: *In order to find the reflexes $\mathcal{R}[k; E](S)$ of a point S on a circle k with respect to the eye point E we have to calculate the roots of an algebraic polynomial of order four $f(x) = \sum_{k=0}^{4} c_k x^k$. With the abbreviations $u = 2/\mathbf{r}^2$, $v = 1/(s_x^2 + s_y^2)$ and $w = 1/\mathbf{e}$ the coefficients of this polynom are*

$$\begin{aligned}
c_4 &= u^2 \\
c_3 &= -2u(vs_x + w) \\
c_2 &= v(1 + 2ws_x) + w^2 - 2u \\
c_1 &= 4s_x v + 2ws_x^2 v + 2w \\
c_0 &= vs_y^2 - v\mathbf{r}^2(1 + 2ws_x + w^2 s_x^2).
\end{aligned} \qquad (5)$$

When parallel projection is applied ($\mathbf{e} = \infty \Rightarrow w = 0$), the formulas (5) reduce to

$$c_4 = u^2,\; c_3 = -2uvs_x,\; c_2 = v - 2u,\; c_1 = 4s_x v,\; c_0 = v(s_y^2 - \mathbf{r}^2). \qquad (6)$$

When S is a point of infinity (polar angle σ, $s_x = s_y = \infty$, $v = 0$), and E is a finite point, the corresponding coefficients are

$$c_4 = u^2,\ c_3 = -2uws_x,\ c_2 = w^2 - 2u,\ c_1 = 2w(1+\cos^2\sigma),\ c_0 = \sin^2\sigma - w^2\mathbf{r}^2\cos^2\sigma. \quad (7)$$

When E and S have the same distance from M, the reflex is known explicitly:

$$R(\pm\mathbf{r}\cos\frac{\sigma}{2}, \pm\mathbf{r}\sin\frac{\sigma}{2}). \quad (8)$$

This is also true for $\mathbf{e} = \overline{MS} = \infty$.

The four solutions of the polynom can be calculated by means of well known formulas ([20])[1]. However, under certain circumstances there are numeric instabilities that may lead to a considerable loss of accuracy. Among the four solutions $\mathcal{R}[k; E](S)$, usually only one is good for practical use. It has to be found "by probe". Note that all four solutions may be practical solutions when the point S is inside k (Fig. 8).

The corresponding y-value is to be determined by (3). In the cylindrical case, the z-values r_z of the corresponding space points $R = \mathcal{R}[\Phi_\zeta; E](S)$ have to be reconstructed via the z-value s_z of S from the "planar solution":

$$r_z = \frac{\overline{ER'}}{\overline{ER'} + \overline{R'S'}} s_z \quad (10)$$

Obviously, the cylindrical reflexes in general are *not* coplanar.

In the spherical case $\mathcal{R}[\Phi_\varkappa; E]$, we have already done our calculations in the plane SEM: Thus, *the spherical reflexes of a point are coplanar*. We have to mention a special case, though: When the point S lies on the axis ME, the connecting plane SEM is not determined uniquely. Two trivial reflexes of S will lie on ME. The spatial position of the two (real or conjugate imaginary) symmetric non-trivial reflexes, however, is not determined uniquely. We thus have the following theorem about the possible degeneration of the set of reflected points:

Theorem 2: *The set $\mathcal{R}[\Phi_\varkappa; E](S)$ contains the two reflexes on ME. When non-trivial real reflexes occur, the reflex additionally consists of a small circle of $\Phi_\varkappa$ with the axis ME.*

We will give an explanation for this strange behaviour when we talk about the reflex of a straight line.

In the following, most considerations will be dedicated to the reflection on the outside of a circle. Then only one of the four theoretical solutions is valid for practical use. This simplifies some theorems, which have to be modified when several practical solutions are allowed.

[1]When less accuracy is necessary and only one solution is of practical use, we can find the particular root of the polynom even a bit faster by means of NEWTON's iteration (we explicitly have the equation of $f'(x)$):

$$x_{n+1} = x_n - \frac{f(x_n)}{f'(x_n)} = x_n - \frac{c_4x_n^4 + c_3x_n^3 + c_2x_n^2 + c_1x_n + c_0}{4c_4x_n^3 + 3c_3x_n^2 + 2c_2x_n + c_1}. \quad (9)$$

After only few iteration steps the x-values practically do not differ from the exact solution.

2.2. "Forbidden regions" and numerical instabilities

Before calculating the reflex of a point, we first have to test whether the reflex is visible or not. Fig. 7 shows the "forbidden region" for the reflection on the outside of the circle. Interpreted three-dimensionally, the area is enclosed by the visible part of the surface and the two tangential planes from E to Φ_ζ or the part of the tangential cone that lies behind the sphere $\Phi_\varkappa$ respectively.

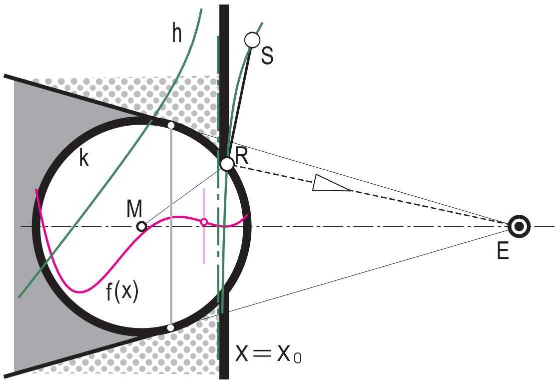

Figure 7: Forbidden region

Numerical problems arise in the neighborhood of

$$x_0 = s_x = \frac{\mathbf{r}}{4\mathbf{e}}(\mathbf{r} \pm \sqrt{\mathbf{r}^2 + 8\mathbf{e}^2}) \tag{11}$$

(Fig. 7, see Section 3, (17)). There the hyperbola degenerates into a pair of straight lines, and two roots of the polynom $f(x)$ are identical. In Fig. 7 the region of the plane to the left of the vertical $x = x_0$ is dotted. For the only reflex R of a point S in this region we always have $r_x > s_x$, whereas for all points to the right of the vertical $r_x < s_x$ is true (reflection on the outside of the circle!).

Because of its essential importance, the corresponding algorithm was especially optimized. We now can calculate approximately $400,000$ reflexes per second (!) with sufficient accuracy on a 500 Mhz PC.

2.3. The catacaustic of the reflection congruence ("circle caustic")

Each tangent at the catacaustic k^* leads to a solution of the reflection problem. Due to the four roots of (5), the catacaustic is a curve of class four. In two special cases the result is well known: When the eye point E is a point of infinity (normal projection), we have a so-called nephroid ([24], Fig. 9 lower right). When E lies on the circle k (this case is only interesting when reflecting on the inside of k), the catacaustic k^* is a cardioid (Fig. 9 lower left). In Fig. 8, the four real tangents at k^* lead to four visible reflexes of a point S inside the circle k (the eye point E is inside the circle as well). When both S and R are outside k, we always have exactly two non-virtual reflexes of S, one for the reflection on the outside of k, one for the reflection on the inside.

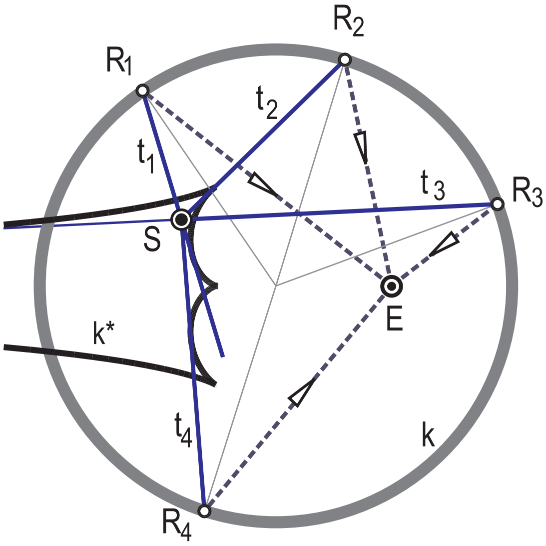

Figure 8: Tangents at k^*

We are now going to calculate the parametric equation and the algebraic properties of k^{*2}. Let the polar angle of R be the parameter φ. When reflecting E at the radial ray through R,

[2] A geometrically interesting approach for the determination of such properties in general was given in [2]. In the special case of the reflection on a circle, the authors quote [3], who may have been the first to detect the corresponding equations.

we get a point $E^*(\mathbf{e}\cos 2\varphi, \mathbf{e}\sin 2\varphi)$. The tangent t at the catacaustic therefore has the parametric equation

$$\vec{x} = \begin{pmatrix} \mathbf{r}\cos\varphi \\ \mathbf{r}\sin\varphi \end{pmatrix} + \lambda \begin{pmatrix} \mathbf{e}\cos 2\varphi - \mathbf{r}\cos\varphi \\ \mathbf{e}\sin 2\varphi - \mathbf{r}\sin\varphi \end{pmatrix} \tag{12}$$

and the parameter-free equation

$$\begin{pmatrix} \mathbf{e}\sin 2\varphi - \mathbf{r}\sin\varphi \\ \mathbf{r}\cos\varphi - \mathbf{e}\cos 2\varphi \end{pmatrix} \vec{x} = \mathbf{er}\sin\varphi.$$

When we intersect t with its derivative $\dot{t}$

$$\begin{pmatrix} 2\mathbf{e}\cos 2\varphi - \mathbf{r}\cos\varphi \\ -\mathbf{r}\sin\varphi + 2\mathbf{e}\sin 2\varphi \end{pmatrix} \vec{x} = \mathbf{er}\cos\varphi,$$

we get the corresponding point on the catacaustic:

$$\begin{pmatrix} 2\mathbf{e}\cos 2\varphi - \mathbf{r}\cos\varphi \\ -\mathbf{r}\sin\varphi + 2\mathbf{e}\sin 2\varphi \end{pmatrix} \left[\begin{pmatrix} \mathbf{r}\cos\varphi \\ \mathbf{r}\sin\varphi \end{pmatrix} + \lambda \begin{pmatrix} \mathbf{e}\cos 2\varphi - \mathbf{r}\cos\varphi \\ \mathbf{e}\sin 2\varphi - \mathbf{r}\sin\varphi \end{pmatrix} \right] = \mathbf{er}\cos\varphi.$$

Thus we have the following parameter for (12):

$$\lambda = \frac{\mathbf{r}^2 - \mathbf{e}\,\mathbf{r}\cos\varphi}{2\mathbf{e}^2 + \mathbf{r}^2 - 3\mathbf{er}\cos\varphi} \tag{13}$$

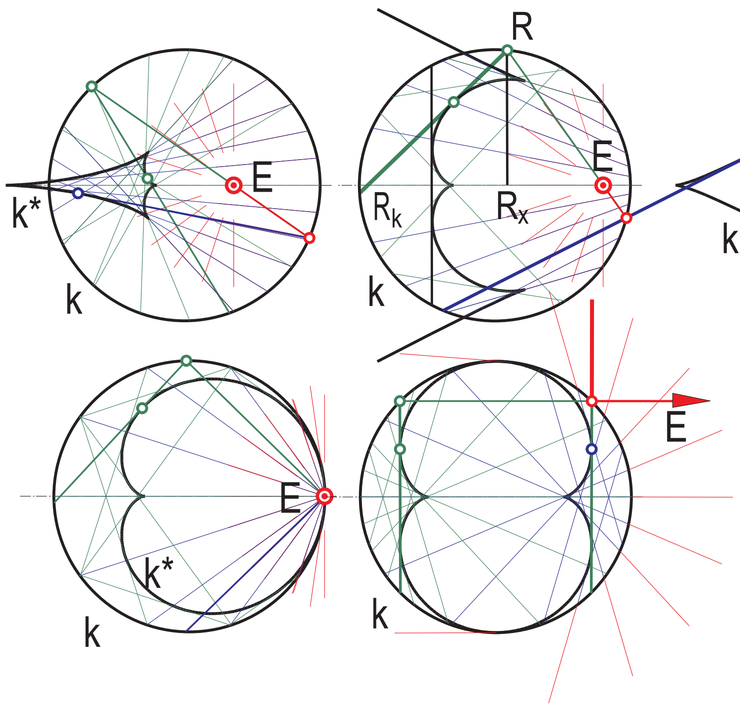

Figure 9: Various catacaustics.

Insertion in (12) and substitution

$$\cos\varphi = \frac{1-t^2}{1+t^2},\ \sin\varphi = \frac{2t}{1+t^2},\ \cos 2\varphi = \frac{1-6t^2+t^4}{(1+t^2)^2},\ \sin 2\varphi = \frac{4t(1-t^2)}{(1+t^2)^2} \tag{14}$$

leads to the following rational parametric equation of the catacaustic k^* (see also [23], [3]):

$$\begin{aligned} x &= \tfrac{1}{\mu}(-\mathbf{r}(t^2+1)^3 - \mathbf{e}(t^2-1)(t^4+10t^2+1)) \\ y &= \tfrac{1}{\mu}16et^3 \\ \text{with } \mu &= \tfrac{\mathbf{e}}{\mathbf{r}}(t^2+1)^3 + 3(t^2-1)(t^2+1)^2 + 2\tfrac{\mathbf{r}}{\mathbf{e}}(t^2+1)^3. \end{aligned} \tag{15}$$

Written in homogenous coordinates $(\mu : x : y)$, the equation shows that in general k^* is of order six. Only for $\mathbf{e} = \mathbf{r}$ the order is reduced to four.

To summarize we can say:

Theorem 3: *When reflecting the rays of a pencil on a circle, the reflected rays envelope curves of class four and order six with the parametric equation* (15)[3].

Fig. 9 shows various forms of the catacaustic. They are all evolutes of the orthonomic of k with respect to E (i.e., a Limacon of Pascal; see [24], [19]). Fig. 10 illustrates how the corresponding catacaustic surfaces are generated by means of translation ($\mathcal{R}[\Phi_\zeta; E]$)) and rotation ($\mathcal{R}[\Phi_\varkappa; E]$).

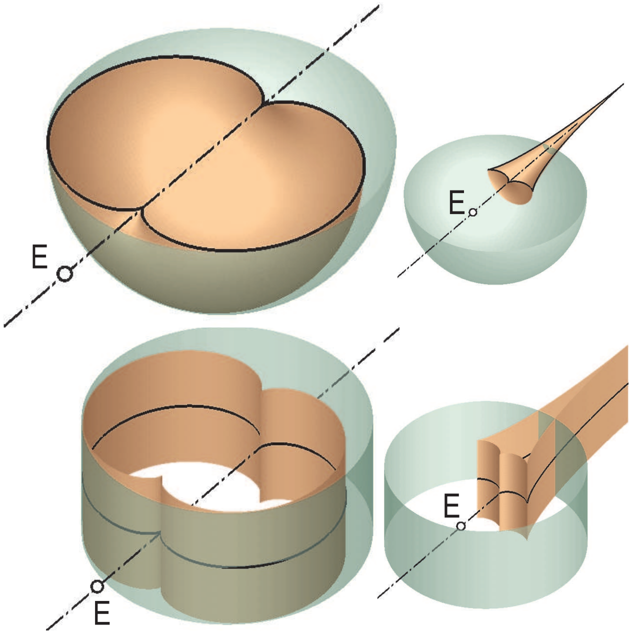

Figure 10: Catacaustic surfaces.

2.4. Anamorphoses

An interesting application of the reflection on a cylinder of revolution — the so-called anamorphoses ([5]), has been known in the arts for a long time (Leonardo da Vinci, Erhard Schön, Hans Holbein d. J.): On the base plane, an image is to be drawn so that it appears undistorted when viewed from an eye point E in a reflecting cylinder of revolution (Fig. 11).

In this case, we project the space point R onto the cylinder (projection center E) and then intersect the corresponding reflected ray with the base plane ($\rightarrow S$). Fig. 11 illustrates the following

Theorem 4: *The reflex of a circle with the cylinder's axis as axis, the radius* $\mathbf{e}$ *and a height difference* Δz *with respect to* E *lies on a parallel circle of the cylinder with height difference* $\Delta z/2$.

This is true because S is the reflex of E' with respect to the cylinder's normal in R' and therefore we have $\overline{SR'} = \overline{R'E'}$. According to (10), we then have the constant value

$$r_z = \frac{\overline{R'E'}}{\overline{SR'} + \overline{R'E'}}\Delta z = \frac{\Delta z}{2}$$

for the height r_z of R.

[3] For practical application, (15) is not appropriate since the distribution of the points is bad and we theoretically need infinite parameters. Instead, we inserted (13) in (12).

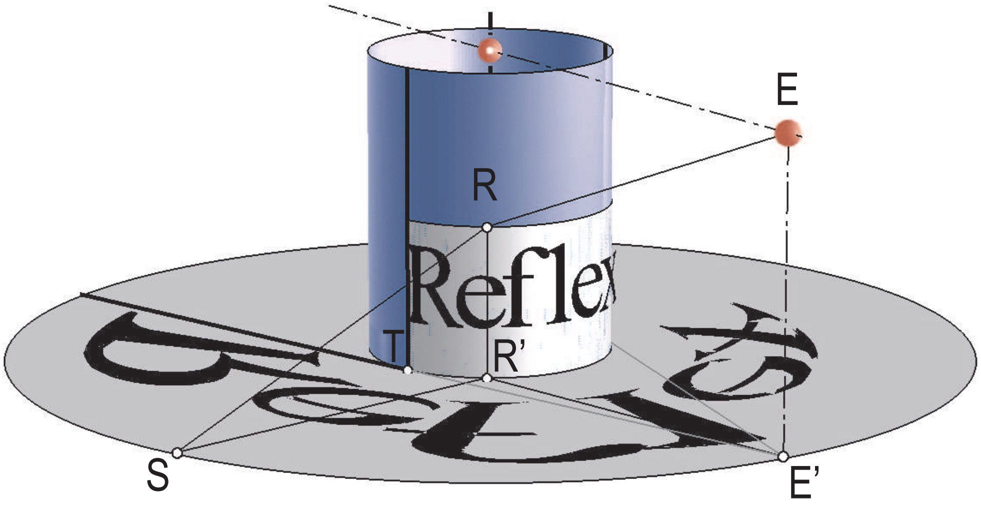

Figure 11: Anamorphosis

2.5. An interesting construction of conics and its "physical consequences"

Geometrically seen, the search for the reflexes of S is identical to the following problem: We consider a linear system of confocal conics with common focuses S and E. We now look for those conics of the system that touch the given circle k (Fig. 12). It is well known that the tangents of a conic are bisectrices of the directrices. It follows that the touching points are the four reflexes of S on k with respect to E. In Fig. 12, the reflexes R_1 and R_2 that belong to the reflection on the outside and the inside respectively lead to ellipses e_1 and e_2, the residual ones to hyperbolas e_3 and e_4 of the pencil. The points R_i again lie on the hyperbola h (Fig. 6).

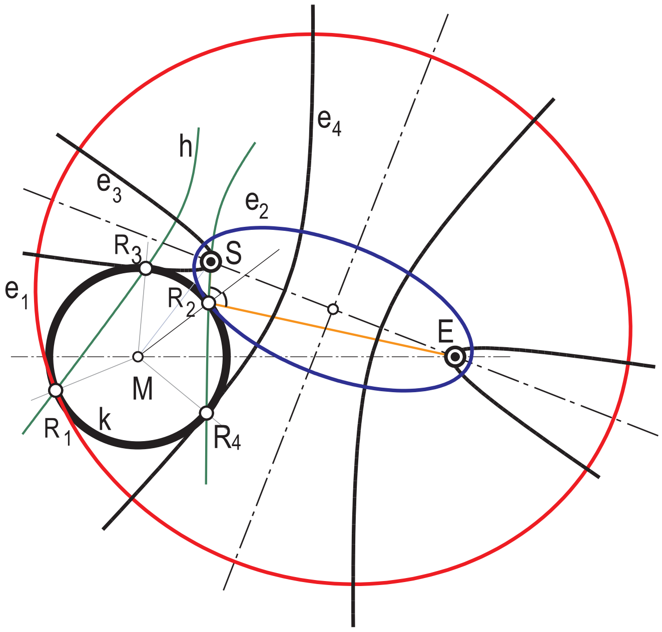

Figure 12: Confocal conics

For $R_i \in e_i$ we have $\overline{ER_i} \pm \overline{SR_i} = 2a_i$ (= const). For points P inside the ellipses e_1 and e_2 we have $\overline{ER_i} + \overline{SR_i} < 2a_i$ and for those outside $\overline{ER_i} + \overline{SR_i} > 2a_i$. Since the circle k touches the ellipse e_1 from the outside and the ellipse e_2 from the inside, the following non-trivial fact holds:

Theorem 5: *Let Φ be a sphere or a cylinder of revolution. When reflecting points outside of Φ, the corresponding distance of the light ray is minimal for the reflection on the outside of Φ. For the reflection on the inside, it is maximal.*

The theorem partly holds for points inside Φ and/or the eye point inside Φ. From now on, we restrict to the reflection on the outside of Φ.

3. Kernel points and kernel planes, reflexes of straight lines

When we intersect the reflected rays (12) with the x-axis, we get points $R_k(x_k, 0)$ for $\lambda = \mathbf{r}/(\mathbf{r} - 2\mathbf{e}\cos\varphi)$ (compare Fig. 5). With $x = \mathbf{r}\cos\varphi$ we have

$$x_k = \frac{\mathbf{e}\mathbf{r}^2}{2\mathbf{e}x - \mathbf{r}^2} \tag{16}$$

which shows that the points R_k and the normal projections R_x of R onto the x-axis are two projective point ranges. This has already been stated in [14], where the points R_k are called "kernel points" and the planes $\varkappa \ni R$ ($\varkappa \perp ME$) are called "kernel planes".

For the double points of the projectivity $R_k \leftrightarrow R_x$ ($x_k = x$) we have

$$x_{1,2} = \frac{\mathbf{r}}{4\mathbf{e}}(\mathbf{r} \pm \sqrt{\mathbf{r}^2 + 8\mathbf{e}^2}). \tag{17}$$

In these two cases the reflected ray t is orthogonal to the axis ME. These rays are the double tangents of the catacaustic k^* (Fig. 9). A comparison with (4) shows that the hyperbola h ((3)) has its intersection points with the x-axis in exactly these points. The given method for the determination of the reflexes gets numerically unstable in the neighborhood of the double points. Since the solution is known for $x = x_{1,2}$, we can easily avoid this instability: All the points on the straight line (17) will have the same reflex on the circle k (reflection on the outside). Interpreted three-dimensionally, this means that for all straight lines in the plane $\varkappa_0$ (17) perpendicular to ME the reflex with respect to Φ lies in $\varkappa_0$: $\mathcal{R}[\Phi_\varkappa; E](b)$ is a small circle of $\Phi_\varkappa$, $\mathcal{R}[\Phi_\zeta; E](b)$ is a generating line of Φ_ζ ([25]).

In the cylindrical case, there is another special case: When a straight line is parallel to the axis of Φ_ζ (i.e., projecting in a top view), its reflex trivially is a generating line of Φ_ζ.

Now to the reflex of a general straight line b on the cylinder Φ_ζ. The manifold of all reflected transversals of b is a ruled surface Ψ of degree four ([14], Fig. 13). The reflex itself is a space curve of order four on this surface. This can be proved analogously to a proof for the spherical case given in [25]: Take a kernel point R_k on the axis $ME = a$. The corresponding kernel plane $\varkappa \ni R$ intersects the cylinder Φ_ζ in the generating line $g \ni R$ (and a symmetrical line).

We now consider two pencils $\mathcal{B}$ and $\mathcal{U}$ of planes through b and the line of infinity u of the kernel planes and declare a projectivity as follows: When a plane $\delta \in \mathcal{B}$ contains the point R_k, the corresponding plane $\overline{\delta} \in \mathcal{U}$ contains R_x (and thus R). The two pencils generate a regulus $\mathcal{R}$ with the generating lines $(\delta \cap \overline{\delta})$. $\delta \supset R_kS \Rightarrow R \in (\delta \cap \overline{\delta}) \Rightarrow R \in \mathcal{R}$. Thus, R lies on $\mathcal{R} \cap \Phi$, which is a space curve of order four (of the "first kind", i.e., it is an intersection curve of two quadrics).

The intersection curve can consist of one or two branches (Fig. 14). When b intersects the axis ME the sphere $\Phi_\varkappa$, the curve degenerates into two circles: One consists of the reflexes of all points of b except the intersection point. The other circular reflex stems from the intersection point on the axis (and can be imaginary) (Theorem 2). For $\mathcal{R}[\Phi_\zeta; E]$, there is no such special case, since the reflexes of a point in general never lie in a plane.

When it comes to the practical calculation of the reflex of a straight line, one should never divide the line into equal distances and then look for the reflexes of the points of division: This way one would get reflexes that are distributed widely exactly where the reflected line is

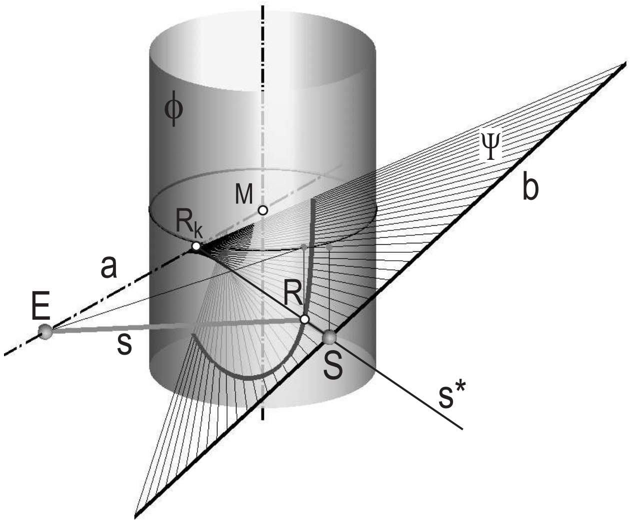

Figure 13: Ruled surface Ψ

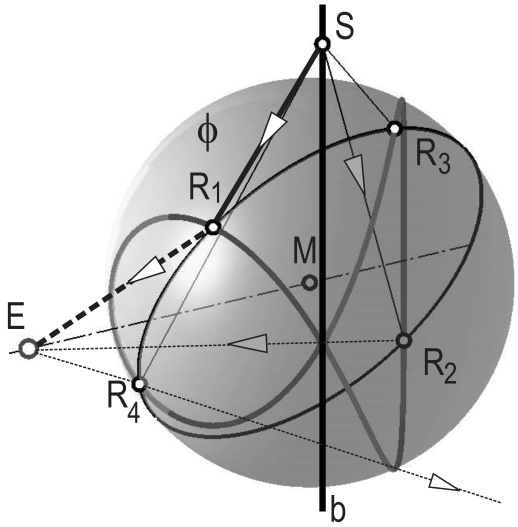

Figure 14: Reflex curve of order four

maximally curved (Fig. 15). In order to find more favorable distances of the knots on the reflex of a straight line, we may proceed as follows: We examine the corresponding two-dimensional situation by projecting b in axis-direction or, in the spherical case, by rotation of the points of b into an auxiliary plane through ME: $b \to b_0$ (in general a hyperbola). We determine the polar angles φ_1 and φ_2 of the end points of the (linear or hyperbolic) segment of b_0. Next we equally subdivide the corresponding arc $[\varphi_1, \varphi_2]$ of the circle k. The reflected rays through these in-between points lead to a set of in-between points on b_0 that have to be transformed back to space. The results (Fig. 16) are satisfying and useful for further spline interpolations.

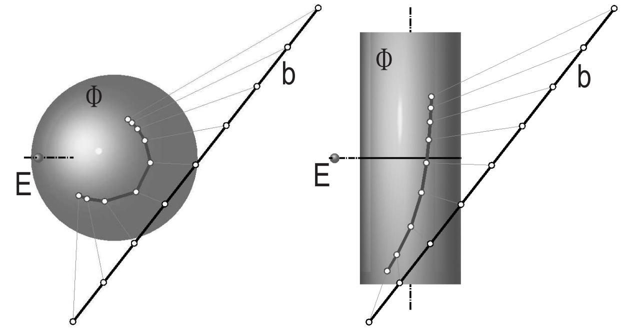

Figure 15: Unfavorable distribution of reflexes

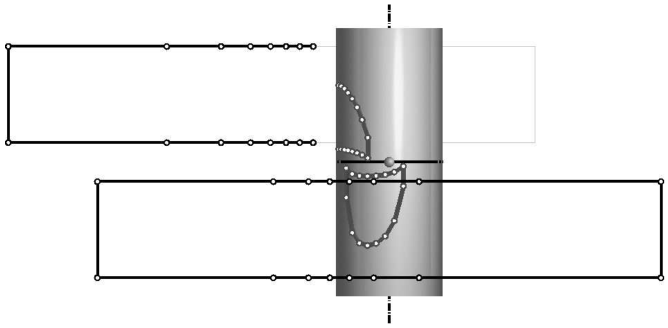

Figure 16: Better distribution

4. Reflexes of polygons

In principle we can now calculate the reflex of a polygon in the following two steps: We first clip the polygon with the borders of the "forbidden areas", thus possibly creating more than one polygon. Secondly, we reflect the sides of the clipped polygon(s) as described above. In most cases, the image of an arbitrary polygon will be non-convex and non-overlapping. When we call the rays that are the reflected rays of the bundle through E "projection rays", we can say: Polygons that are seen "one-sided" will not have overlappings.

In order to determine whether possible overlappings occur like in Fig. 17 and Fig. 18, we can proceed as follows: The polygon's carrier plane β intersects the reflecting cylinder of revolution in an ellipse, the reflecting sphere possibly in a small circle c. The reflected rays of all points $C \in c$ generate a ruled surface Ψ. When there are generating lines of Ψ in β, they and only they will lead to the "multiple points" of the polygon. We thus have

Theorem 6: *The reflex of a polygon will for sure not overlap when the polygon's plane β does not intersect the reflecting surface Φ, or when in all points of the intersecting curve c the oriented reflected half-rays are on the same side of β.*

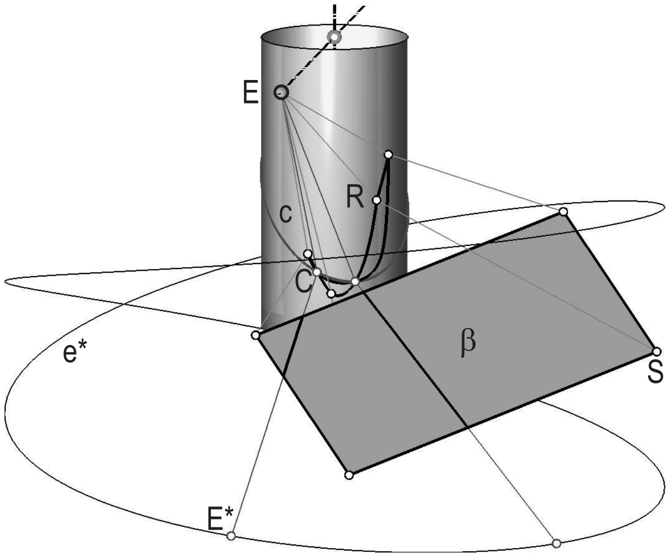

Figure 17: Overlapping polygon on Φ_ζ

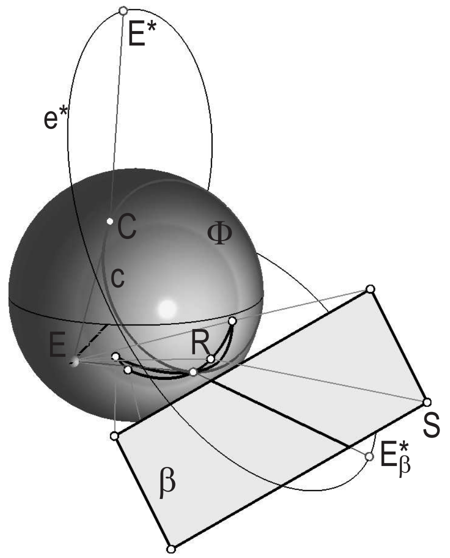

Figure 18: Overlapping polygon on $\Phi_\varkappa$

In Fig. 17 and Fig. 18, the oriented reflected half-rays on the ruled surface Ψ were intersected with a coaxial cylinder through the eye point E, or a concentric sphere through E, respectively. Without proof, they are "Umschwungkurven" e^* of order four ([16]). The intersection points $E^*_\beta = e^* \cup \beta$ lead to the double points on c.

We first consider the reflection on a cylinder of revolution Φ_ζ: Let

$$z = ax + by + d \tag{18}$$

be the equation of β (we can exclude the case that β is parallel to the cylinder's axis, because then we either do not have an intersection curve or the reflected surface Ψ consists of two planes). Then, a general point on the intersection ellipse $c = \Phi_\zeta \cap \beta$ has the coordinates

$$C(\mathbf{r}\cos\varphi, \mathbf{r}\sin\varphi, a\mathbf{r}\cos\varphi + b\mathbf{r}\sin\varphi + d). \tag{19}$$

We now reflect the ray ES on Φ_ζ and consider a point E^* on the new ray with $\overline{CE^*} = \overline{CE}$:

$$\overrightarrow{E^*}(\mathbf{e}\cos 2\varphi,\ \mathbf{e}\sin 2\varphi\, 2(ar\cos\varphi + b\mathbf{r}\sin\varphi + d)) \tag{20}$$

We have $E^* \in \beta$ when the condition

$$2(a\mathbf{r}\cos\varphi + b\mathbf{r}\sin\varphi + d) = a\mathbf{e}\cos 2\varphi + b\mathbf{e}\sin 2\varphi + d$$

is fulfilled. With the substitution

$$u = \mathbf{r}\cos\varphi \ (\Rightarrow \mathbf{r}\sin\varphi = \sqrt{\mathbf{r}^2 - u^2},\ \mathbf{e}\cos 2\varphi = \frac{\mathbf{e}}{\mathbf{r}^2}(2u^2 - \mathbf{r}^2), \mathbf{e}\sin 2\varphi = \frac{2\mathbf{e}}{\mathbf{r}^2}u\sqrt{\mathbf{r}^2 - u^2}) \quad (21)$$

we have an algebraic equation of order four $g(u) = \sum_{k=0}^{4} g_k u^k$. Its coefficients are (with the abbreviation $v = a^2 + b^2$):

$$\begin{aligned} g_4 &= \mathbf{e}^2 v \\ g_3 &= -2\mathbf{e}\mathbf{r}^2 v \\ g_2 &= \mathbf{r}^2(\mathbf{r}^2 v - \mathbf{e}^2 v - ade) \\ g_1 &= \mathbf{r}^4(ad + a^2\mathbf{e} + 2b^2\mathbf{e}) \\ g_0 &= \tfrac{\mathbf{r}^4}{4}(a^2\mathbf{e}^2 + d^2 + 2ad\mathbf{e} - 4b^2\mathbf{r}^2). \end{aligned} \quad (22)$$

We finally have

Theorem 7: *When reflecting a polygon in the plane* (18) *on a cylinder of revolution, the reflex has no overlappings when the algebraic equation of order four* (22) *has no real roots. If real roots u_i occur, they lead via the parameter $\varphi_i = \pm\arccos\frac{u_i}{\mathbf{r}}$ to points C_i on the ellipse* (19) *and E_i^* on the curve* (20). *When the line $C_iE_i^* \subset \beta$ intersects the outline of the polygon, the polygon has an overlapping and is to be split.*

Clearly, points C_i on the "invisible" side of the cylinder can be neglected.

Now to the reflection on a sphere $\Phi_\varkappa$: By means of a rotation about the x-axis through an angle θ, the polygon's plane β can be transformed into a z-parallel position β_0:

$$ax + by = d \quad \text{with} \quad \sqrt{a^2 + b^2} = 1 \quad (23)$$

This plane intersects the sphere $\Phi_\varkappa$ only for $|d| \le \mathbf{r}$. The intersecting circle $c_0 = \Phi \cap \beta_0$ is given by its center $N_0(ad, bd, 0)$ and its radius

$$r_0 = \sqrt{\mathbf{r}^2 - d^2}. \quad (24)$$

It can be parametrized as follows:

$$\vec{c_0} = \begin{pmatrix} ad - br_0\cos\varphi \\ bd + ar_0\cos\varphi \\ r_0\sin\varphi \end{pmatrix} = \begin{pmatrix} ad - bu \\ bd + au \\ \pm\sqrt{r_0^2 - u^2} \end{pmatrix} \quad (\text{with } r_0\cos\varphi = u). \quad (25)$$

In order to find points $E_0^* \in e_0^*$, we reflect E on the sphere's normal through C_0:

$$\vec{e_0^*} = \begin{pmatrix} \lambda(ad - bu) - \mathbf{e} \\ \lambda(bd + au) \\ \pm\lambda\sqrt{r_0^2 - u^2} \end{pmatrix} \quad \text{with} \quad \lambda = \frac{2\mathbf{e}}{\mathbf{r}^2}(ad - bu) \quad (26)$$

The intersection of e_0^* and c_0 leads to the linear(!) equation

$$u = \frac{2ad^2\mathbf{e} - \mathbf{r}^2(a\mathbf{e} + d)}{2bd\mathbf{e}}. \quad (27)$$

Provided $u < r_0$, i.e.,

$$\frac{2ad^2\mathbf{e} - \mathbf{r}^2(a\mathbf{e} + d)}{2bd\mathbf{e}} < \sqrt{\mathbf{r}^2 - d^2} \tag{28}$$

we get via (27) two straight lines $\overline{C_0E_0}$ that are symmetrical with respect to the plane $z = 0$: We have to insert (27) into (25) and (26), respectively. Again, points C_0 on the "invisible" part of the sphere can be neglected. The straight lines $\overline{C_0E_0}$ are finally to be rotated into the polygon's plane β (about the x-axis through $-\theta$). When they intersect the polygon, the polygon is to be split.

To sum up:

Theorem 8: *When reflecting on a sphere $\Phi_\varkappa$, the reflex of a polygon does not overlap when it's carrier plane does not intersect $\Phi_\varkappa$. Otherwise, the reflex can have up to two overlappings when condition* (28) *is fulfilled.*

Finally a practical hint: When a polygon is very small, a test is not necessary. When it comes to the reflection of *large or long polygons*, however, one should definitely perform the above described test (and split the polygon if necessary), because the result of the filling of a polygon with overlappings is usually unpredictable.

Those straight lines in the polygon's plane β that appear "projecting", can be called "contour" of β in a wider sense. We have

Theorem 9: *The "contour" of a plane consists of a maximum of four points when reflecting on a cylinder of revolution, and a maximum of two points, when reflecting on a sphere.*

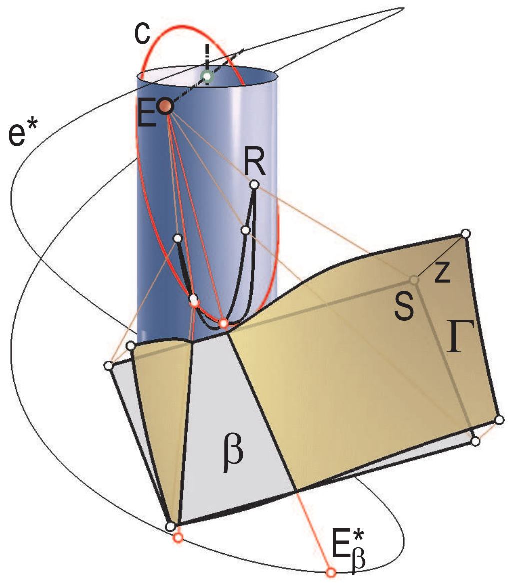

Figure 19: Function graph Γ above β

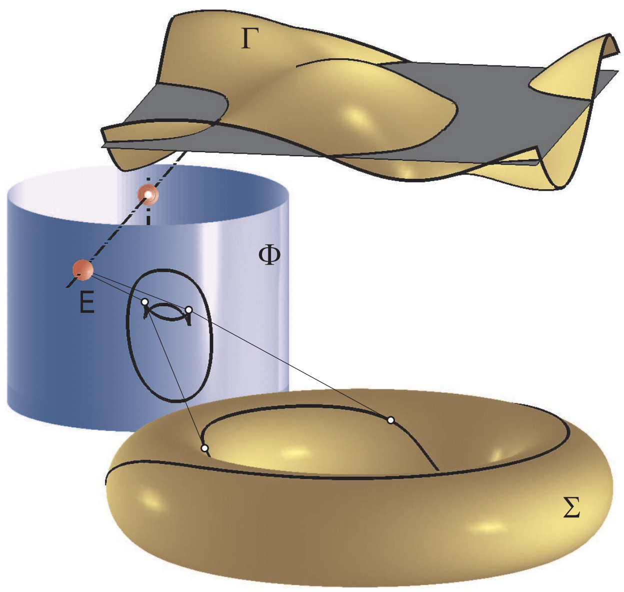

Figure 20: "Reflex contour"

Another possibility to test whether a polygon has overlappings or not — which is more of theoretical interest rather than for practical use — is the following: We define a function graph Γ above the polygon, the points of which lie on the normal to the carrier plane β. The "height" z of the point equals the dot product of the normal vector of β and the direction vector of the corresponding reflected ray through the base point (Fig. 19). The zero manifold of Γ is then either empty ($\Rightarrow$ no overlappings) or it consists of the above described reflected rays in β. This method is of course much more computation expensive as the one described in Theorem 6 or Theorem 8 respectively. It can, however, be generalized in order to calculate contours of mathematically defined surfaces. By the way, Fig. 19 illustrates that a polygon sometimes has to be split even when the reflected oriented half rays through all its vertices are on the same side of its carrier plane β.

5. Reflex-contours of parameterized surfaces

Let Σ be a parameterized surface

$$\vec{x}(u,v) \quad \text{with} \quad u \in [u_1, u_2], v \in [v_1, v_2]. \tag{29}$$

We now define a function graph Γ above the rectangular area $u_1 \le u \le u_2,\ v_1 \le v \le v_2$: The z-value corresponding to a point (u, v) is

$$z = \vec{n}\vec{s}. \tag{30}$$

Thereby $\vec{n}$ is the normalized normal vector in the point $\vec{x}(u,v) \in \Sigma$, and $\vec{s}$ is the normalized direction vector of the corresponding "projection ray" (Fig. 20). Γ and Σ are one-to-one correspondent. The zero manifold of Γ leads to those points of Σ, the tangent planes of which are "projecting" and thus lie on the reflex contour.

Theorem 10: *The reflex contour of a parameterized surface Σ corresponds to the zero manifold of a function graph with the equation (30).*

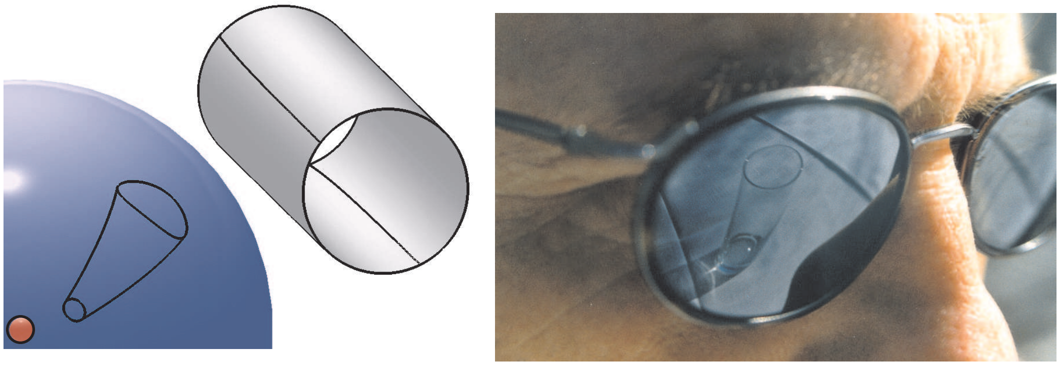

Figure 21: Reflection of a cylinder on a sphere

When efficient algorithms are applied ([8]), reflex contours of curved surfaces can be calculated in comparatively short periods of time (approximately 1-3 frames per second on a 500 *Mhz* PC).

As an additional example, Fig. 21 shows the reflection of a cylinder of revolution on a sphere. Note that the curves on the cylinder that lead to the reflex contour are of course not straight lines. The image to the left is computer generated, the one to the right is a photographic image of the reflection in (spherical) sun glasses.

6. Conclusion and future work

We have seen that reflections on very specific surfaces like cylinders of revolution and spheres can be treated successfully by adapted mathematical methods rather than by the application of very general rendering algorithms. Especially the explicit knowledge of the catacaustic surfaces of the reflection congruence can be very useful for the understanding of otherwise hard-to-explain special effects.

Some questions, however, remain for future work:

- How can the above mentioned special surfaces be generalized so that the given formulas can still be used? E.g., general canal surfaces (like surfaces of revolution or tubular surfaces) are enveloped by a set of spheres. The reflexes of a point can thus be found iteratively by means of auxiliary spheres.
- The explicit knowledge of the position of specular points on surfaces of revolution or general canal surfaces allows an adapted triangulation of the surface. This helps to render such surfaces photo-realistic by means of hardware-supported GOURAUD-shading. In fact, we can now shade spheres and cylinders of revolution – including specular points — in real time and without the use of ray tracing.
- We can efficiently create curved perspectives by means of reflections on cylinders of revolution and spheres. They are very useful when we want to see “as much as possible” in an ultra-wideangle perspective ([10]). There are still some problems, though: How can existing hardware be used in order to speed up hidden-surface algorithms? A general approach in this direction has been examined in [18].
- Refractions and reflections seem to be closely related. E.g., it can be shown that the caustics are very similar. There is even a possible correspondence between refractions and reflections. Refractions are already used for the creation of ultra-wideangle perspectives (fish-eye objectives!)

I have to thank W. FUHS and H. P. SCHRÖCKER for valuable discussions about the topic.

References

[1] J. ARVO: *Backward Ray Tracing.* SIGGRAPH ’86 Developments in Ray Tracing course notes, 1986.

[2] J.W. BRUCE et al.: *On caustics of plane curves.* American Mathematical Monthly **88**, no. 9, 651–667 (1981).

[3] A. CAYLEY: *A memoir upon caustics.* Philos. Trans. Roy. Soc. London **147**, 273–312 (1857): Collected Works, vol. 2., 336–380.

[4] M. COHEN, J.R. WALLACE: *Radiosity and Realistic Image Synthesis.* Academic Press, 1989.

[5] J. ELFFERS et al.: *Anamorphosen — Ein Spiel mit der Wahrnehmung, dem Schein und der Wirklichkeit.* DuMont Buchverlag, Köln 1981.

[6] W. BAIER: *Optik, Perspektive und Rechnung in der Photographie.* Fachbuchverlag, Leipzig 1959.

[7] A. GLASSNER (ed.): *An Introduction to Ray-Tracing.* Academic Press, 1989.

[8] G. GLAESER: *Fast Algorithms for 3D-Graphics.* Springer N.Y., 1994.

[9] G. GLAESER, H. STACHEL: *Open Geometry.* Springer N.Y., 1999.

[10] G. Glaeser: *Extreme and curved perspectives.* Topics in Algebra, Analysis and Geometry, 1999, pp. 39–51.

[11] H. Gouraud: *Continuous shading of surfaces.* IEEE Transactions on Computers June 1971 C-20(6), pp. 223–228.

[12] H. Hollein: *Haas-Haus.* `www.greatbuildings.com/buildings/Haas_Haus.html`.

[13] H. Holditch: *On the n-th Caustic, by Reflexion from a Circle.* Quart. J. Math. **2**, 301–322 (1858).

[14] H. Horninger: *Zur geometrischen Theorie der Spiegelung an krummen Oberflächen.* Sitzungsber., Abt. II, österr. Akad. Wiss., Math.-Naturw. Kl. **145**, 367–385 (1936).

[15] M. Inakage: *Caustics and Specular Reflection Models for Spherical Objects and Lenses.* The Visual Computer **2**, no. 6, 379–383 (1986).

[16] W. Kautny: *Zur Geometrie des harmonischen Umschwungs.* Montsh. Math. **60**, 66–82 (1956).

[17] P. M. Neumann: *Reflections on Reflection in a Spherical Mirror.* American Mathematical Monthly **105**, no. 6, 523–528 (1998).

[18] E. Ofek, A. Rappoport: *Interactive reflections on curved objects.* Computer Graphics **26**, no. 2 (SIGGRAPH '98 proceedings), 333–342 (1998).

[19] H. Sachs, G. Karáné: *Schall- und Brechungsfronten an ebenen Kurven.* Publ. Math. Debrecen **54**, 189–205 (1999).

[20] J. Schwarze: *Cubic and Quartic Roots.* In Graphics Gems (A. Glassner (ed.), Academic Press, 1990, pp. 404–407.

[21] C. Ucke, C. Engelhardt: *Kaustik in einer Kaffeetasse.* Physik in unserer Zeit **29**, 120–122 (1929).

[22] M. Watt: *Light-Water Interaction using Backward Beam Tracing.* Computer Graphics **24**, no. 4 (SIGGRAPH '90 Proceedings), 377–385 (1990).

[23] E.W. Weisstein: *CRC Concise Encyclopedia of Mathematics.* CRC Press, 1998, `www.treasure-troves.com/math`.

[24] H. Wieleitner: *Spezielle ebene Kurven.* Sammlung Schubert XLI, G.J. Göschen, Leipzig 1908.

[25] W. Wunderlich: *Darbouxsche Verwandtschaft und Spiegelung an Flächen zweiten Grades.* Deutsche Math. **7**, 417–432 (1943).

Received July 28, 1999; final form November 9, 1999